Investigation on the competing effects of clay dispersion and matrix plasticisation for polypropylene/clay nanocomposites. Part I: Morphology and mechanical properties

Yu Dong [a,*], Debes Bhattacharyya [b]

[a] *Department of Mechanical Engineering, Curtin University of Technology*
GPO Box U1987, Perth, WA 6845, Australia
[b] *Centre for Advanced Composite Materials, Department of Mechanical Engineering*
The University of Auckland, Private Bag 92019
Auckland, New Zealand

Abstract

The key compatibiliser role of maleated polypropylene (MAPP) to improve the clay dispersability has been explicitly addressed in the fabrication process and material characterisation of polypropylene (PP)/clay nanocomposites. However, its matrix plasticiser role, which has been rarely mentioned, could adversely influence the excellent mechanical properties of such nanocomposites, resulting from the homogeneous clay dispersion. PP/clay nanocomposites in the presence of MAPP were prepared by twin screw extrusion and subsequently injection moulded with three typical material formulations in fixed parametric settings: (1) weight ratio (WR) of clay and MAPP, WR=1:2; (2) MAPP content of 6 wt% and (3) clay content of 5 wt%. The morphological structures and mechanical properties of PP/clay nanocomposites were examined by using X-ray diffraction (XRD) analysis, transmission electron microscopy (TEM), scanning electron microscopy (SEM) and universal mechanical testing. The further improvement of mechanical properties was evidently hindered with very inconsiderable alteration of morphological structures in terms of the clay dispersion level. This observation could be ascribed to the change of MAPP role from a compatibiliser to a plasticiser due to its excessive amount used above a certain

* Corresponding author. Tel.: +61 8 92669055; fax: +61 8 92662681.
E-mail address: Y.Dong@curtin.edu.au (Y. Dong).

saturation level, which was found in range of 3-6 wt% in MAPP contents for the enhancements of tensile and flexural properties of PP/clay nanocomposites.

Keywords: Nanocomposites; nanoclays; maleated polypropylene; matrix plasticisation; mechanical properties; morphological structures

1. Introduction

The pioneering work on the synthesis of nylon 6/clay nanocomposites with excellent mechanical properties [1] has inspired engineers and material scientists to significantly involve such key polymer nanocomposite research field on how to uniformly disperse the clay nanoplatelets into continuous polymers. Manufactures of polymer/clay nanocomposites predominantly benefit from the essential advantages of superior mechanical, thermal, barrier and flame retardant properties [1-7]. However, it is of great concern to the material engineering community from a vast range of polymers to select the cheap, multifunctional and recyclable one. The enormous applications for automotive and packaging industries have led to recent commercial interests on PP/clay nanocomposites. This focused trend inevitably arises from material merits of common commodity polymer PP in light weight, low cost, good balance of chemical and physical properties and excellent processibility. Current fabrication techniques of PP/clay nanocomposites using twin screw extrusion, in-situ polymerisation and solution casting have only allowed for a partially intercalated and exfoliated clay formation, thus in lack of experimentally complete exfoliation. From the industrial and commercial point of view, the implicit nexus between the enhancement of their mechanical properties, especially the stiffness and strength, and corresponding morphological structures is still worthwhile to be investigated in a more systematic manner.

In order to develop PP/clay nanocomposites as the replacement of conventional fibre composites with superior mechanical properties, there are at least two critical issues to be solved [8]. The first one is to separate the stack-layered clay particles in the PP matrix to

significantly broaden the interlayer spacing and eventually peel the individual clay platelets apart (i.e. full exfoliation). The second is to facilitate the active interfacial interactions and achieve the great compatibility between clay particles and the PP matrix. Both aspects rely heavily on the suitable compatibilisers such as maleated PP (MAPP) with functional polar groups. Early research work by Hasgawa et al. [9] shows that the stiffness of PP/clay nanocomposites continues to increase with the additional MAPP content up to 20 wt%. Nevertheless, initial controversial studies by Lee et al. [10], Chow et al. [11] and Dong et al. [12] indicate that a competing effect due to the clay dispersion and MAPP matrix plasticisation might affect the mechanical properties of prepared nanocomposites with a certain threshold for the MAPP saturation level, beyond which the property enhancement diminishes. Furthermore, it has also been reported by Gicía-López et al. [13] and Dong et al. [12, 14] that impact strengths of PP/clay nanocomposites continuously decreased in excess of MAPP. As a consequence, it is crucial to distinguish the compatibiliser or plasticiser role of MAPP for making a better property enhancement balance on nanocomposite counterparts.

The purpose of this study is to investigate the matrix plasticisation effect of MAPP on the resulting mechanical properties of PP/clay nanocomposites in relation to the clay dispersion during the morphological characterisation so that the saturation level of compatibilisers can be determined as the material formulation guidance to nanocomposite manufacturers.

2. Experimental Details

2.1 Materials

PP homopolymer H380F (density: 0.9 g/cm^3, melt flow index MFI=25 g/10 min at 230°C and 2.16 kg) was supplied by Clariant (New Zealand) Ltd and MAPP Exxelor™ PO1020 (MA content: 0.5-1 wt%, MFI= ~ 430 g/10 min at 230°C and 2.16 kg) was selected as the compatibiliser obtained from ExxonMobil Chemical (Germany).

NANOLIN™ DK4 organomodified clay (density: 1.8 g/cm^3 and interlayer spacing: d_{001} = 3.56 nm) modified with octadecylammonium salt was purchased from Zhejiang Fenghong Clay Chemicals, Co. Ltd, China. This type of organoclay is in form of fine white powders with the average fully dispersed clay platelet thickness about 25 nm (aspect ratio: 100-1000) in 95-98% purified smectite content.

2.2 Nanocomposite preparation and formulations

PP/clay nanocomposites were prepared based on melt compounding PP and MAPP pellets with the downstream clay feeding by using a co-rotating intermesh twin screw extruder Brabender® DSE20 (screw diameter: D = 20 mm and L:D = 40:1) at 185-210°C with a screw speed of 200 rpm. Subsequently, the initially prepared nanocomposites were recompounded to extend the residence time at a relatively low speed of 100 rpm. Raw materials and collected nanocomposites were dried in a vacuum oven at 90°C for over 16 hrs. The final nanocomposite pellets were further injection moulded to make material testing samples using a BOY 50A machine at 190-210°C at the die temperature of 25°C and injection pressure of 60-80 bars. The material preparation procedure was described in details elsewhere [12].

In this study, three typical material formulations of PP/clay nanocomposites are listed in Table 1. Type I is a mathematically well-balanced formulation on the basis of preferred combination of factors determined from the previous Taguchi design of experiments (DoE) [12]. Type II with the fixed MAPP content of 6 wt% is selected from the economic point of view to reduce the MAPP usage cost and simultaneously consider the effect of clay content. Type III evaluates the effect of MAPP content on the mechanical properties of nanocomposites with respect to the matrix plasticisation. All the formulations are subjected to the similar processing conditions mentioned earlier.

2.3 Characterisation methods

XRD analysis was performed at room temperature using a Bruker D8 ADVANCE diffractometer which was operated at 40 kV and 40 mA with Cu-k_α X-ray beam (wave length λ = 0.15406 nm). The XRD patterns were scanned at 2θ = 2-10° (scan rate: 0.4°/min). The XRD samples were obtained either directly from the raw clay powders or cut into strips from the injection moulded tensile samples of neat PP and formulated nanocomposites subjected to the subsequent hand polishing with sandpaper. The interlayer spacing (d_{001}) of clay platelets was then determined from the 2θ position of the clay (001) basal reflection peak based on Bragg's law ($n\lambda=2d_{001}sin\theta$) as a similar case for d_{002} and d_{003} in the corresponding clay (002) and (003) reflections. Moreover, a basic peak fitting analysis was also made based on the Gaussian distribution function to smooth the original XRD patterns.

To further examine the intercalated/exfoliated structures with respect to the clay dispersion, TEM analysis was conducted on the ultrathin nanocomposite samples (nominal thickness: 70 nm) with a Philips CM12 transmission electron microscope at an accelerating voltage of 120 kV. Such TEM samples were cryogenically microtomed in the melt flow direction at -80°C using a Hitachi S-4700 ultramicrotome and were then collected on 300 mesh copper grids.

The fracture morphology and clay dispersion were also investigated by a Philips XL30S Field Emission Gun scanning electron microscope at 5.0 kV. A strip-like section was taken from the middle portion of a tensile sample and notched parallel to the longitudinal tensile direction using a hacksaw, which was quenched in liquid nitrogen and cryogenically ruptured prior to the platinum sputter coating.

Mechanical properties were determined by using tensile, flexural and impact tests according to ASTM D638, D790 and D6110, respectively. Tensile testing was carried out on a universal tensile machine Instron® 1185 at room temperature. The chord tensile

modulus (0.05-0.25% strains) with an extensometer (gauge length: 50 mm) at a crosshead speed of 5 mm/min and the tensile yield strength at 50 mm/min were measured accordingly. The flexural testing was performed using a laboratory-scaled three-point bending rig on the Instron® 1185 with the chord flexural modulus (0.05-0.25% strains) and flexural strength (calculated from 5% strain) determined at a speed of 1.22 mm/min. The Charpy impact strength was obtained by breaking notched injection moulded impact samples using a CEAST® Resil 25 pendulum impact testing machine. Before the mechanical testing conducted, samples were dried in a silica gel-contained vacuum desiccator for over 24 hrs. The reported results are based on the average data of over five samples with calculated standard deviations.

3. Results and Discussion

3.1 Determination of intercalation effect

XRD patterns of three typical formulations of PP/clay nanocomposites are compared to investigate the intercalation effect in the clay dispersion, as depicted in Fig.1. The calculated interlayer spacing values ($d_{001,}$ $d_{002,}$ d_{003}) are reported in Table 2. Apparently, DK4 organoclay possesses three distinct (001), (002) and (003) diffraction peaks at 2.48, 4.88 and 7.36°, which correspond to the interlayer spacings of 3.56, 1.81 and 1.20 nm, respectively. Regardless of used material formulations, the positions of (001), (002) and (003) peaks did not alter considerably and peak intensities were reduced accordingly due to the break-down mechanism of clay tactoids into finer particles using twin screw extrusion. Such low increase level of interlayer spacing might be attributed to the nature of organomodified DK4 in surface treatment with relatively high d_{001} = 3.56 nm as opposed to untreated natural clay silicates (d_{001} = 0.96 nm) [15]. In addition, the use of DK4 clays could result in the limited intercalation in well-ordered clay structures. Therefore, the further enhanced interlayer spacing becomes quite difficult to achieve without an optimised extrusion process.

In formulation Type I, the first peaks are gradually shifted to low diffraction angles when decreasing the clay content, Fig. 1(a). The interlayer spacings of nanocomposites are reported to increase from 3.62 (Opt4) to 3.73 nm (Opt1) in contrast to 3.56 nm for DK4 organoclay, implying the existence of limited intercalated clay platelets. However, the intensities of first peaks are gradually enhanced with increasing the clay content, which suggests that large well-ordered clay tactoids still occur in PP/clay nanocomposites at a high clay content level. The second and third reflection peaks show the similar tendency though the XRD peaks have been broadened with decreasing the clay content. As expected, this observation can be due to the fact that clay tactoids are separated into much thinner stacks of layered clay structures with some possible exfoliation formation.

In formulation Type II, the first diffraction peaks of PPNC3 and PPNC5 again tend to be shifted to the lower angles with intercalated structures by having the interlayer spacings decreased from 3.73 to 3.58 nm accordingly, Fig. 1(b). Unfortunately, beyond the clay content of 5 wt%, the threshold effect takes place with the peak shifting to the higher angles in PPNC8 and PPNC10, leading to the reductions of interlayer spacing to 3.53 and 3.50 nm, respectively. From the material processing point of view, the decrease of interlayer spacing can result from the compaction of clay particles in the twin screw extrusion especially when handling the higher clay content with the possibility of clay agglomeration. Hence the slight clay collapse structures could occur during the melt compounding of PP/clay nanocomposites. Moreover, the low thermal stability of clay intercalated structures may also be responsible for such interlayer spacing reduction. Since melt compounding has been conducted at relatively high temperatures above 180°C, interlayer surfaces of DK4 organoclay present less organophilic characteristics in view of thermodynamic interaction. This case can be explained by the release of organic molecules by the thermal decomposition of organic/inorganic surfactants like thermal desorption of organic ion and thermal decomposition of organic molecule itself [16]. More remarkably,

the first peak intensities for PPNC5, PPNC8 and PPNC10 become relatively low compared to those for corresponding Opt2, Opt3 and Opt4 at the same clay contents, indicating that more disordered and random-oriented clay dispersion have been achieved by breaking up clay tactoids into clay platelets with micro/nanostructures in formulation Type II. Additionally, peak broadening phenomenon is also observed in the second and third diffraction peaks despite identical interlayer spacings of PPNC8 and PPNC10 to that of DK4 organoclay.

With respect to formulation Type III, it appears that there is no noticeable (001) peak intensity reduction as the MAPP content increases, which implies that the increase of MAPP content has little influence on the further break-down of clay particles. Without the presence of MAPP, the first peak of MAPP0 is shifted to the higher diffraction angle compared to that of DK4 organoclay, resulting in the decrease of interlayer spacing to 3.52 nm, Fig. 1(c). Such phenomenon has greatly diminished when MAPP is used beyond 6 wt%, which demonstrates that the compatibiliser, along with the threshold effect, plays a major role in the enhanced interlayer spacing due to the effective intercalation. To a great extent, the presence of MAPP alleviated the clay collapse structure and surfactant degradation owing to the thermal decomposition as mentioned earlier. In particular, MAPP10 achieves the highest interlayer spacing of 3.70 nm for the first peak, as compared to 3.62 nm for MAPP20. This result also confirms that the excessive amount of low molecular weight MAPP might not further promote the interlayer expansion during the intercalation, which has been well interpreted according to the effective intercalation mechanism [12]. The second and third peaks of MAPP10 show the peak shifting to the lower angles with the corresponding slightly larger interlayer spacings of 1.88 and 1.25 nm as compared to 1.81 and 1.20 nm for DK4 organoclay, respectively. Nevertheless, a very minor alteration has been found for the remaining nanocomposites, which is the case for MAPP0, MAPP3. MAPP6 and MAPP20.

The peak width and intensity observed in XRD pattern do not suffice to accurately quantify the particle size and thickness of clay platelets due to their high sensitivities to the sample preparation, orientation and processing conditions [17, 18]. Since XRD analysis is mainly used to detect the interlayer spacing of well-ordered stacks of layered structure of clay platelets, a supplementary technique like TEM analysis is essential to compensate for the lack of observation for delaminated/exfoliated and highly heterogeneous intercalated structures [19]. Consequently, apart from the clay collapse structure in formulation Type II and III, it is still at an early stage to infer that the clay dispersion and material properties are completely detrimental due to the more complex morphological structures to be further determined by TEM.

3.2 TEM morphological characterisation

The TEM micrographs of PP/clay nanocomposites are exhibited in Figs. 2 and 3 at ×15000 magnification with arrows indicating the major orientation directions of clay particles. Such orientation demonstrates the well-ordered nature of DK4 organoclays in either aggregated or limited intercalated forms within PP/clay nanocomposites, as also evidenced in appearance of relatively high (001) peak intensities irrespective of material formulation types.

In formulation Type I, a good clay dispersion can be clearly seen especially at low clay contents of 3 and 5 wt%, Figs. 2(a) and (b), and a mixed morphological structure with the combination of intercalated stacks and exfoliated platelets are very manifested. However, clay platelets in the lateral dimension of 200-500 nm appear in skewed and curved structures with some degree of localised random orientation despite the apparent overall major orientations, possibly resulting from the core effect of nanocomposite samples prepared by injection moulding process [15]. At the higher clay contents of 8-10 wt%, apart from some extent of typical clay tactoids, the clay dispersion has been greatly improved and becomes reasonably uniform, Fig. 2(c) and (d). It appears that the presence

of MAPP helps to reduce the agglomeration size of clay particles owing to its effective compatibiliser role.

As for formulation Type II, the uniform clay dispersion with partial intercalation/exfoliation formation can still be obtained below the clay content of 5 wt%, Figs. 2(a) and (e). Nonetheless, an increasing number of intercalated stacks of clay particles inevitably become much thicker with the existence of more clay aggregates beyond 1μm at higher contents (8-10 wt%), Figs. 2(f) and (g). More importantly, a wide range of clay dispersion level for the morphological structures occurs from almost exfoliated (2-3 platelet thick), highly intercalated (>10 nm) particles to large tactoids as opposed to the prevalent intercalation with a less variation of particle size in formulation Type I. This TEM finding reveals that instead of intercalation, the collapse structure of clay platelets due to the previous decreased interlayer spacing values might be partially influenced by unhomogenised clay particles consisting of large tactoids.

The effect of MAPP content on the clay dispersion level in formulation Type III is illustrated in Fig. 3. When MAPP is not contained in the nanocomposite formulation, typical clay tactoids at a microscale level (>2 μm) have been widely detected, Fig. 3(a). However, some mixed intercalated clay platelets are still visible, which lies in the physical shearing mechanism in twin screw extrusion. In the presence of MAPP, the sizes of clay tactoids are significantly reduced and multiple intercalated clay platelets along with some individual exfoliated platelets are formed instead, Figs. 3(b)-(e). As expected, the degree of dispersion and the exfoliation level are enhanced with increasing the MAPP content. When the MAPP content is beyond 6 wt%, the morphological structures indicate that the clay dispersion level has not been considerably improved even though the higher MAPP content of 20 wt% provides slightly better dispersion, Figs. 3(c)-(e), which coincides with the XRD results in Fig.1(c) having unnoticeably reduced peak intensities. This finding implies that an optimal amount of MAPP might be fulfilled, and beyond that, MAPP could not further

promote the compatibility between clay particles and the PP matrix, but more or less acts as a part of the PP matrix to soften overall nanocomposites.

3.3 SEM microstructural analysis

The fracture morphology of PP/clay nanocomposites using SEM analysis were also investigated in Figs. 4-6. It can be seen that the original DK4 organoclay is prone to clustering in platelet stacks with a particle size of less than 30 μm, Fig. 4(a). Considering the fracture surfaces of formulation Type I, a good clay dispersion with localised clay tactoids (< 2 μm) has been observed, particularly for Opt1 and Opt2 with the clay contents of less than 5 wt%, Figs. 4(b) and (c). When increasing the clay content up to 8-10 wt%, the great extent of clay agglomeration does not evidently appear, which can result from the dual favourable effects of compatibiliser MAPP and large interlayer spacing of DK4 organoclay, Figs. 4(d) and (e). The large interlayer spacing contributes to much weaker van der Waals forces to facilitate the separation of clay tactoids on the condition that a sufficient amount of MAPP is incorporated in the clay interlayers to achieve the good compatibility. Therefore the majority of large DK4 organoclay particles are broken up into clay platelets in size of 500 nm-1μm.

On the other hand, at the fixed MAPP content of 6 wt% in Type II, to understand the effect of clay content on the fracture morphology of PP/clay nanocomposites, it is found that PPNC3 and PPNC5 again reveal a similar uniform clay dispersion, benefiting from the small amount of clay inclusions though visible clay tactoids still locally coexist, Figs. 4(b) and 5(a). However, large clay tactoids around 2-3 μm are clearly displayed at high clay content levels of 8-10 wt%, which are mixed with already separated clay platelets (300-500 nm in lateral dimensions), Figs. 5(b) and (c). Despite the difficult quantification of the extent of clay tactoids, it is quite convincing that they play a very dominant role in the fracture morphology due to the poor compatibility in lack of MAPP content to enhance the clay separation/delamination, as opposed to the higher clay amounts in PPNC8 and

PPNC10. More interestingly, a great number of cavity-like voids also appear mainly on the fracture surfaces of PPNC8 and PPNC10, which is believed to be originally embedded with clay tactoids/platelets prior to cryofracturing. Such voids with an average size of 2 μm also demonstrate a characteristic of fracture brittleness compared to the fracture ductility observed in neat PP. Most likely, those voids were produced due to the similar debonding effect in the conventional fibre composites. It also confirms that the poor interfacial adhesion takes place especially between clay tactoids and the PP matrix. This observation highlights the importance of sufficient MAPP content to allow for better interfacial interactions which are essential for the effective stress transfer in PP/clay nanocomposites.

Finally as shown in formulation Type III, without the compatibiliser MAPP, the micrograph of MAPP0 in Fig. 6(a) indicates that the PP matrix is surrounded mostly with uncompatibilised large clay tactoids of around 2-3 μm apart from a reasonable clay dispersion. Apparently, the interfacial areas either present partially embedding effect with small gaps between clay particles and the PP matrix or completely become aforementioned cavity-like voids, signifying very weak interfacial interactions in the absence of MAPP. With increasing the MAPP content, the clay particle size is significantly reduced and clay tactoids are separated into much thinner clay platelets with a greatly improved interfacial adhesion, as is the case for MAPP3, MAPP6, MAPP10 and MAPP20 shown in Figs. 6(b), 5(a), 4(c) and 6(c), respectively. It is also seen that the higher the MAPP content is, the finer clay dispersion and smaller clay particle size are shown, typically in the micrographs of MAPP3 and MAPP20, Figs. 6(b) and (c).

Overall, SEM analysis, to a certain extent, detects a mix of micro/nanostructures ranging from aggregated clay tactoids to separate clay platelets in all formulated PP/clay nanocomposites which reflect the different levels of clay dispersion and interfacial interactions in the fracture morphology.

3.4 Mechanical properties

Mechanical properties of PP/clay nanocomposites in formulation Type I and II are illustrated in Fig. 7. In Type I, tensile and flexural moduli are significantly improved with increasing the clay content, as compared to those of neat PP, Figs. 7(a) and (c). With 10 wt% DK4 organoclay, the maximum enhancements of tensile and flexural moduli reach 41 and 61%, respectively. More noticeably, there is a sharp increasing trend in flexural modulus for a very low clay content (< 3 wt%), followed by a much slower increase (3-5 wt%) and more steady increase beyond 5 wt% while the tensile modulus appears in a relatively monotonic increasing manner. The tensile and flexural strengths also increase by maximum 16 and 22%, respectively. Remarkable strength increasing trends are consistently observed for clay contents less than 3 wt%, Figs. 7(b) and (d). But beyond this threshold, they become more or less level-off irrespective of the clay content. The better tensile and flexural properties might be attributed to a higher level of intercalated/exfoliated structures in the clay dispersion and better improvement of the interfacial adhesion, especially for the low clay content (≤ 5 wt%). The strength level-off effect at high clay contents (8-10 wt%) might be explained by a proportional increase of MAPP content (weight ratio of DK4 organoclay and MAPP, WR=1:2) to promote the clay dispersion and delamination in compensation for the negative effect of clay agglomeration. Furthermore, apart from the appearance of some microvoids, good interfacial interactions maintain reasonably well between dispersed clay platelets and the PP matrix. Accordingly, at higher clay contents, the presence of MAPP seems to favour the clay intercalation into PP molecular chains and stabilise the tensile/flexural strength at an acceptable level, higher than or similar to that of neat PP, depending on the interfacial interactions [20]. It is also worth mentioning that the flexural properties of such nanocomposites always demonstrate greater enhancements than the corresponding tensile properties, which could be attributed to the different deformation mechanisms using tensile and bending modes and the

alignment of clay platelets in the PP matrix owing to the injection moulding process [21]. The influence of clay content on the relevant impact properties is depicted in Fig. 7(e). Initially, with an increase of clay content, the Charpy impact strength is drastically enhanced by the maximum 50% when increasing up to 3 wt% organoclay and then drops off in a similar manner until it levels off at a high clay content of about 10 wt%, which is comparable to that of neat PP. The higher impact strength at a low clay content possibly benefits from more uniform clay dispersion leading to the better intercalation/exfoliation level. The reduction of impact strength often occurs at a high clay content due to the induced material brittleness from the proportional amount increases of organoclay and MAPP owing to the more brittleness nature of MAPP than neat PP itself.

On the other hand, identical enhancement trends for tensile and flexural moduli have also been detected for formulation Type II with increasing the clay content. More surprisingly, even higher modulus enhancements take place beyond 3 wt% organoclay compared to those for Type I. In particular, such an increasing tendency appears to be much more pronounced for tensile modulus. It is reported that the highest levels of modulus enhancements again occur at 10 wt% organoclay with 60 and 68% increases for tensile and flexural moduli, respectively. The improvements of tensile and flexural strengths become even more favourable for Type II with a similar level-off effect beyond 5 wt% organoclay. The tensile and flexural strengths show the maximum enhancements up to 21 and 35% with corresponding 5 and 8 wt% organoclay. The flexural strength offers a higher enhancement level as opposed to flexural modulus while vice versa for the tensile properties. The variation of enhancement levels again can be due to the deformation mechanisms and the level of exfoliation/intercalation. Generally, increasing the amount of MAPP leads to the improvement of clay dispersion with better delamination and interfacial interactions. But it is not always the case for the resulting enhancement of mechanical properties. Overall, formulation Type II reveals better tensile and flexural properties

compared to Type I with even higher MAPP contents. It is not surprising owing to the matrix plasticisation effect arising from the low molecular weight MAPP as the compatibiliser. In general polymer blending process, the saturation level of compatibiliser content is a crucial factor, beyond which the homogeneity and mechanical properties of blended materials can be worsened [11, 22, 23]. Up to the saturation level, short molecules of the compatibiliser exist primarily in the interfacial area between dispersed phase and the matrix. But above this level, only a portion of the molecules enter the interfacial area, and the excessive amount of compatibiliser is dispersed in the matrix, thus adversely influencing its homogeneity and then the mechanical properties of blended materials. In fact, the actual amount of MAPP required for improving the interfacial interactions in formulation Type I might be much less than the quantity initially added. The excessive quantity of MAPP only leads to its less effective functionality as a compatbiliser (likely becoming a part of PP matrix), thus lowering the overall material properties. As mentioned earlier, the clay agglomeration in existence of microvoids from Type II at high clay contents (8-10 wt%), in the other way, reveals the weak interfacial interactions owing to the insufficient MAPP content. Consequently, a well-balanced compatibiliser content is essential for the effective melt compounding of PP/clay nanocomposites. As a compromise in practice, tensile and flexural properties in Type I might relatively suffer from the predominant negative MAPP plasticisation effect in competition with the better clay dispersion [17, 24, 25]. The corresponding impact strengths resemble those in Type I up to the clay content of 5 wt% and then follow a relatively slow decreasing tendency until up to 10 wt% where the impact strength is just slightly lower than that of neat PP. The less amount of MAPP may reduce the deterioration of impact strength at the given clay content beyond 5 wt% since a higher MAPP content increases the possibility of multiple short molecular chain branching of the compatibiliser and restricts its penetration into the

polymer phases, thus leading to the material inhomogeneity and adversely influencing the impact strength [22].

For better understanding the saturation level of MAPP content, mechanical properties of PP/clay nanocomposites in formulation Type III are exhibited in Fig. 8. Tensile and flexural moduli inevitably increase with the addition of MAPP up to 3 wt%, but subsequently tend to be reduced while reaching 10 wt% MAPP, Figs. 8 (a) and (b). Then they become more or less level-off at the higher MAPP content levels (10-20 wt%) apart from slight variations, depending on the measured properties. With respect to tensile and flexural strengths, the maximum enhancements have been found to be over 7 and 12% (MAPP content: 3-6 wt%), respectively, as compared to those without MAPP. Hence, the saturation level of MAPP content is estimated to be in the range of 3-6 wt% where both tensile and flexural properties reach the highest levels. In a practical case, the saturation level chosen at a given MAPP content might not always offer the maximum modulus and strength values simultaneously to achieve well-balanced properties, as seen in Fig. 8(b). Meanwhile, the tensile and flexural properties at a higher MAPP content (10-20 wt%) appear to be almost comparable to those without MAPP due to the aforementioned matrix plasticisation effect. However, the property enhancements of PP/clay nanocomposites are still manifested compared to those of neat PP. As expected, the impact strength is greatly reduced with increasing the MAPP content, Fig. 8(c). But at a lower MAPP content (0-3 wt%), the higher level of impact strength is maintained with over 61% increase compared to that of neat PP. This result might benefit from the usage of a small amount of MAPP in polymer blending for the improvement of interfacial interactions, inducing less material inhomogeneity as well as less brittle behaviour. More noticeably, at a higher MAPP content (approximately 17-20 wt%), the impact strength of such nanocomposites is even lower than that of neat PP. As a result, any further increase of MAPP content gradually

worsens the impact strength, which again could due to the less functionality of MAPP as the compatibiliser.

4. Conclusions

The material formulations and characterisation of PP/clay nanocomposites with respect to the competing effects of clay dispersion and matrix plasticisation have been successfully investigated. In the evaluation of intercalation effects, both intercalated and clay collapse structures are shown using XRD analysis. The collapse structure might be ascribed to the clay compaction at higher content levels as well as the thermal decomposition. TEM characterisation further confirms that the formation of partially intercalation/exfoliation in PP/clay nanocomposites occurs at the clay content of less than 5 wt%. Formulation Type I shows more prevalent intercalated clay platelets while Type II provides a wide range of clay particles from individually exfoliated, highly intercalated to clay tactoids especially at high clay contents of 8-10 wt%. As observed in Type III, the clay dispersion level is found to be greatly improved by increasing MAPP content with a threshold effect, above which the further improvement becomes trivial. The SEM analysis also indicates that very uniform clay dispersion normally takes place in fracture morphology at the low clay content (< 5 wt%). The clay agglomeration with the cavity-like microvoids are more evident at higher clay content of 8-10 wt%, especially for Type II, which represents the poor compatibility due to the lack of MAPP content and the weak interfacial interactions. Increasing the MAPP content in Type III leads to the finer clay dispersion with a greatly improved interfacial adhesion. Mechanical properties of PP/clay nanocomposites, as a whole, are remarkably enhanced compared to those of neat PP. However, they are influenced not only by the clay dispersion but also by the functionality of MAPP as the compatibiliser to enhance the interfacial interactions while simultaneously reduce the matrix plasticisation effect, which normally occurs in general polymer blending process. From the viewpoint of using economical materials, it is very clear that the

selection of a relatively small amount of MAPP should be more favourable provided that both the negative effects of matrix plasticisation and clay agglomeration can be successfully controlled in PP/clay nanocomposite compounding to an acceptable level.

Acknowledgements

The authors sincerely acknowledge research financial supports from the Tertiary Education Commission (TEC), New Zealand to Dr. Yu Dong through Bright Future Top Achiever Doctoral Scholarship and the Foundation for Research, Science and Technology (FRST funding # UOAX 0406), New Zealand.

References

[1] Okada A, Kawasumi M, Usuki A, Kojima Y, Kurauchi T, Kamigaito O (1990) In: Schaefer DW, Mark JE (ed) Polymer based molecular composites, MRS Symposium Proceedings, Pittsburgh, USA, 171, p. 45-50.

[2] Giannelis EP (1996) Adv Mater 8: 29-35.

[3] Giannelis EP (1998) Appl Organomet Chem 12: 675-680.

[4] Kojima Y, Usuki A, Kawasumi M, Okada A, Fukushima Y, Kurauchi T, Kamigaito O (1993) J Mater Res 8: 1185-1189.

[5] Messersmith PB, Giannelis EP (1995) J Polym Sci Part A 33: 1047-1057.

[6] Gilman JW (1999) Appl Clay Sci 15: 31-49.

[7] Vaia RA, Price G, Ruth PN, Nguyen HT, Lichtenhan J (1999) Appl Clay Sci 15: 67-92.

[8] Oya A (2000) In: Pinnavaia TJ, Beall GW (ed). Polymer-clay nanocomposites. John Wiley &Sons, New York, p. 151-172.

[9] Hasegawa N, Kawasumi M, Kato M, Usuki A, Okada A (1998) J Appl Polym Sci 67: 87-92.

[10] Lee EC, Mielewski DF, Baird RJ (2004) Polym Eng Sci 44: 1773-1782.

[11] Chow WS, Mohd Ishak ZA, Karger-Kocsis J, Apostolov AA, Ishiaku US (2003) Polymer 44: 7427-7440.

[12] Dong Y, Bhattacharyya D (2008) Compos Part A 39: 1177-1191.

[13] Gicía-López D, Picazo O, Merino JC, Pastor JM (2003) Eur Polym J 39: 945-950.

[14] Dong Y, Bhattacharyya D, Hunter PJ (2008) Compos Sci Technol 68: 2864-2875.

[15] Fornes TD, Paul DR (2003) Polymer 44: 4993-5013.

[16] Wee JW, Lim YT, Park OO (2000) Polym Bull 45: 191-198.

[17] Mittal V (2007) J Thermoplast Compos Mater 20: 575-599.

[18] Lee H, Fasulo PD, Rodgers WR, Paul DR (2005) Polymer 46:11673-11689.

[19] Morgan AB, Gilman JW (2003) J Appli Polym Sci 87 :1329-1338.

[20] Alexandre M. Dubois P (2000) Mater Sci Eng 28: 1-63.

[21] Chow WS, Bakar AA, Mohd Ishak ZA, Karger-Kocsis J, Ishiaku US (2005) Eur Polym J 41: 687-696.

[22] Sathe SN, Rao GSS, Rao KV, Devi S (1996) Polym Eng Sci 36: 2443-2450.

[23] Sathe SN, Devi S, Rao GSS, Rao KV (1996) J Appl Polym Sci 61: 97-107.

[24] Kim DH, Fasulo PD, Rodgers WR, Paul DR (2007) Polymer 48: 5308-5323.

[25] Osman MA, Rupp JEP (2005) Macromol Rapid Commun 26: 880-884.

List of Figures

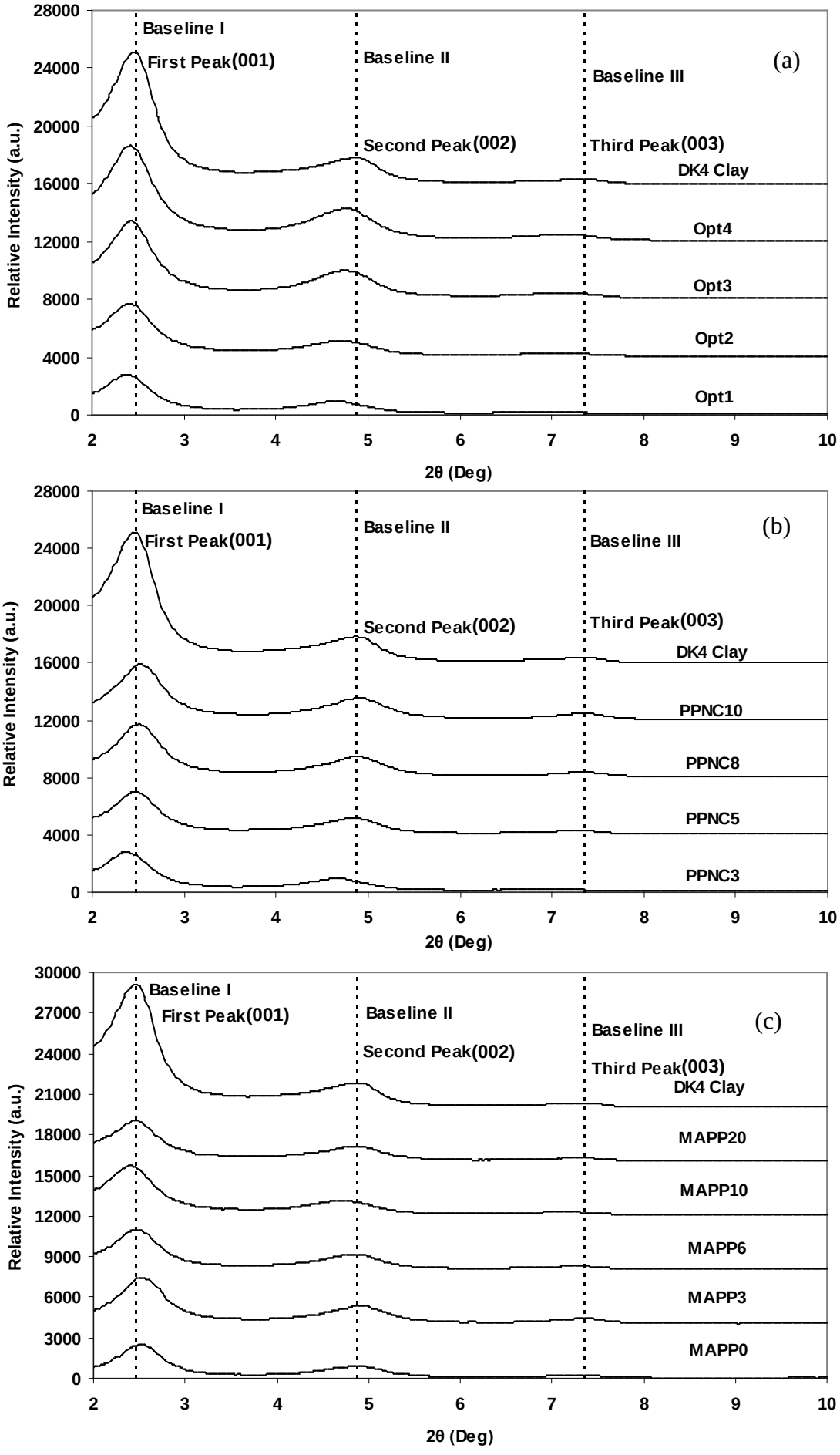
Baseline I
First Peak(001)
Baseline II
Second Peak(002)
Baseline III
Third Peak(003)
(a)
DK4 Clay
Opt4
Opt3
Opt2
Opt1
Relative Intensity (a.u.)
2θ (Deg)
(b)
PPNC10
PPNC8
PPNC5
PPNC3
(c)
MAPP20
MAPP10
MAPP6
MAPP3
MAPP0

Fig.1

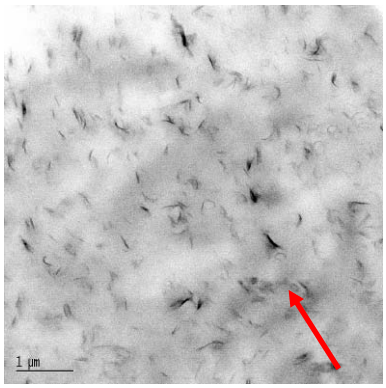

(a)

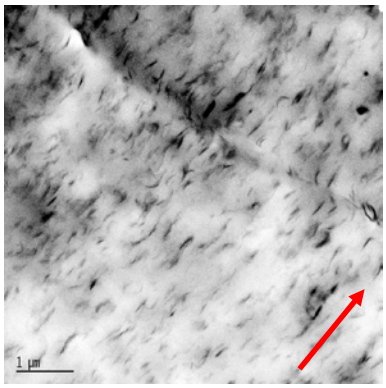

(b)

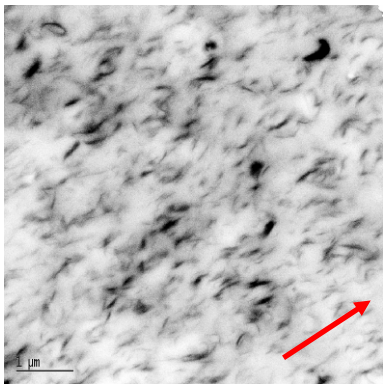

(c)

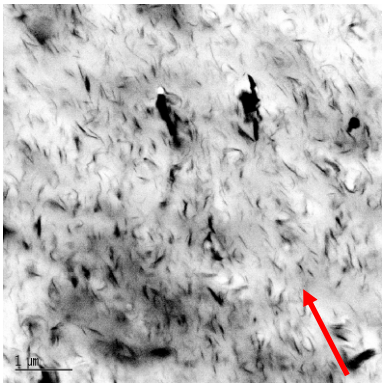

(d)

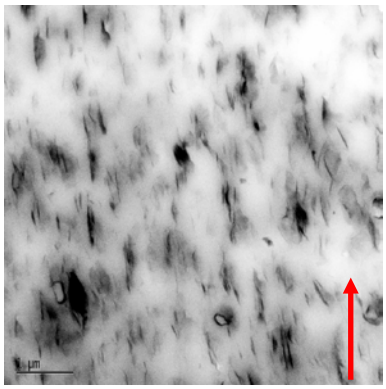

(e)

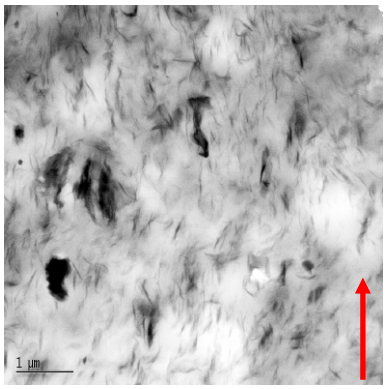

(f)

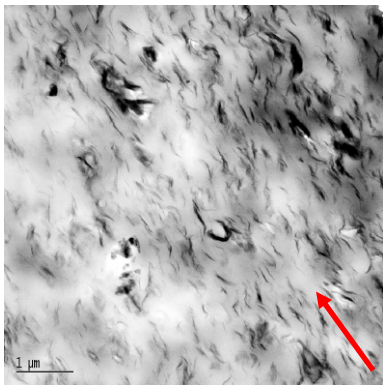

(g)

Fig.2

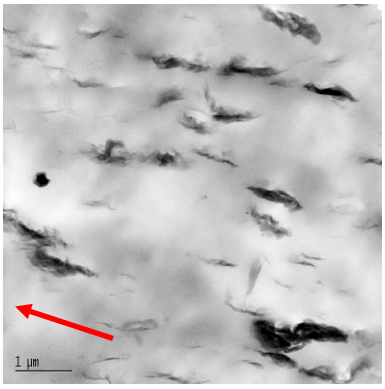

(a)

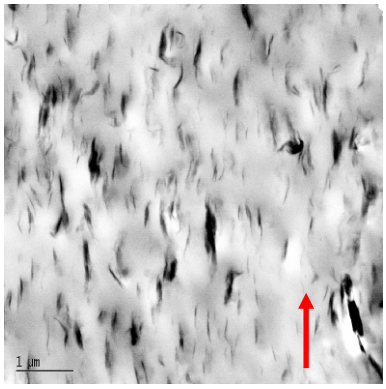

(b)

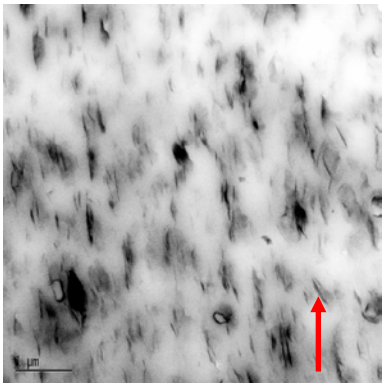

(c)

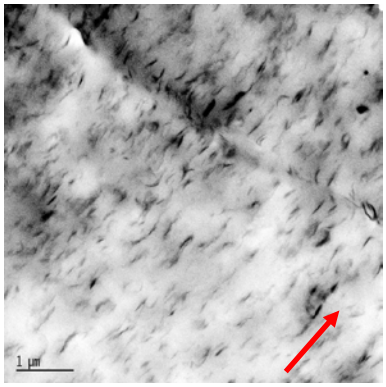

(d)

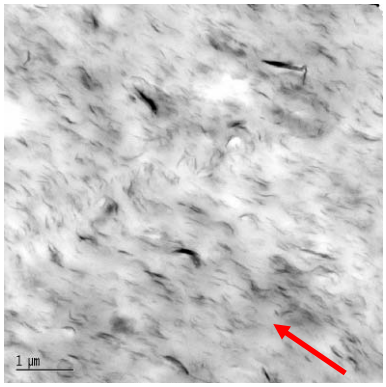

(e)

Fig.3

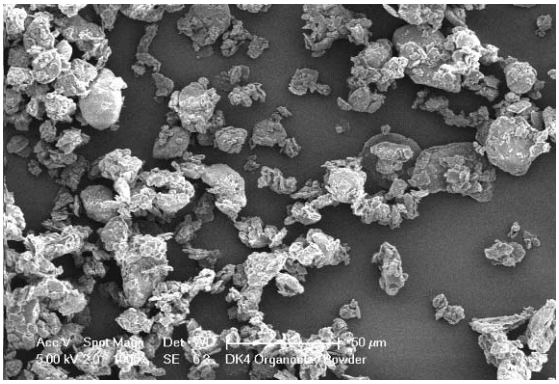
Acc.V Spot Magn Det WD 50 μm
5.00 kV 2.0 SE DK4 Organoclay Powder

(a)

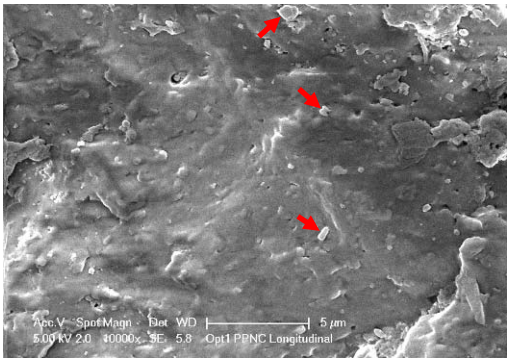
Acc.V Spot Magn Det WD 5 μm
5.00 kV 2.0 10000x SE 5.8 Opt1 PPNC Longitudinal

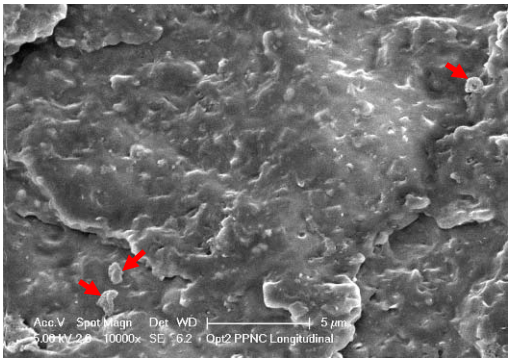
Acc.V Spot Magn Det WD 5 μm
5.00 kV 2.0 10000x SE 6.2 Opt2 PPNC Longitudinal

(b) (c)

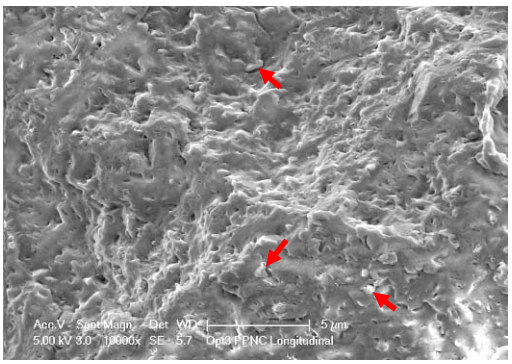
Acc.V Spot Magn Det WD 5 μm
5.00 kV 3.0 10000x SE 5.7 Opt3 PPNC Longitudinal

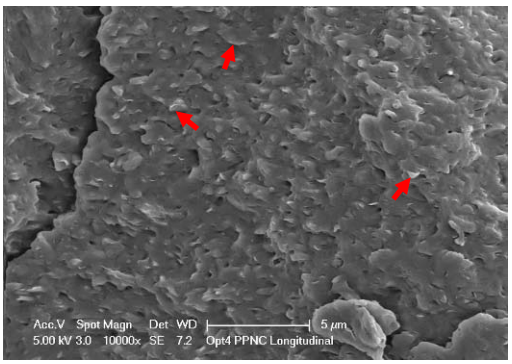
Acc.V Spot Magn Det WD 5 μm
5.00 kV 3.0 10000x SE 7.2 Opt4 PPNC Longitudinal

(d) (e)

Fig.4

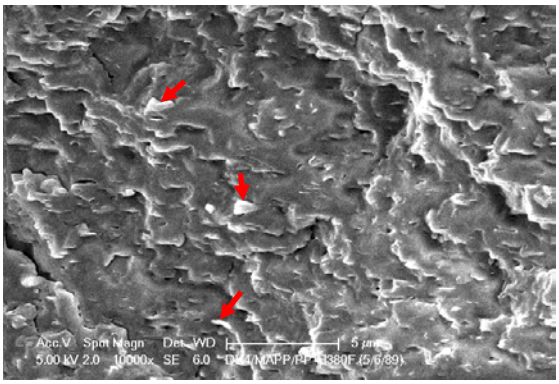

(a)

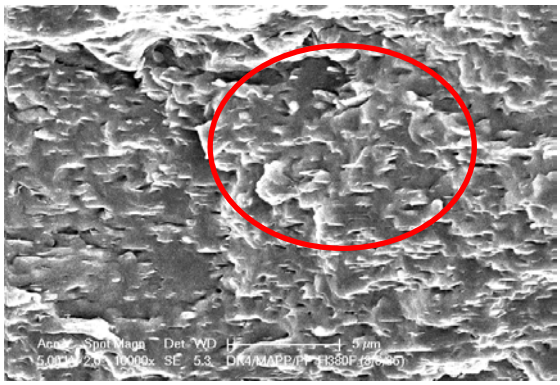

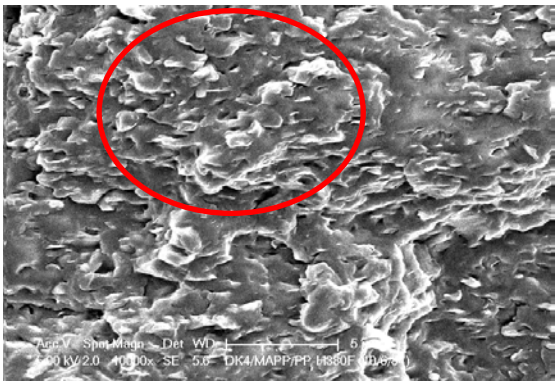

(b) (c)

Fig.5

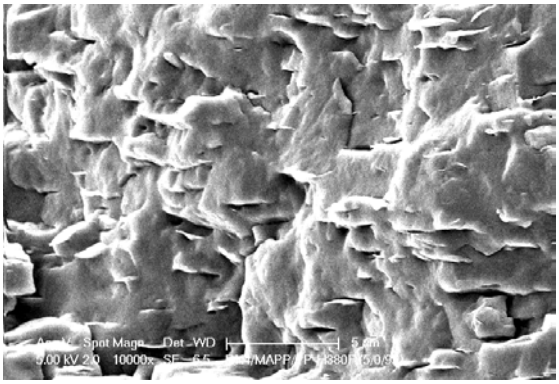

(a)

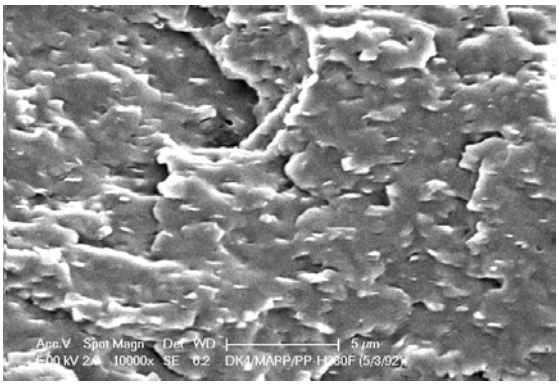

(b)

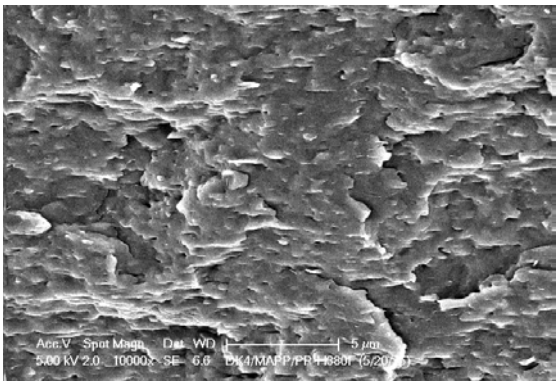

(c)

Fig.6

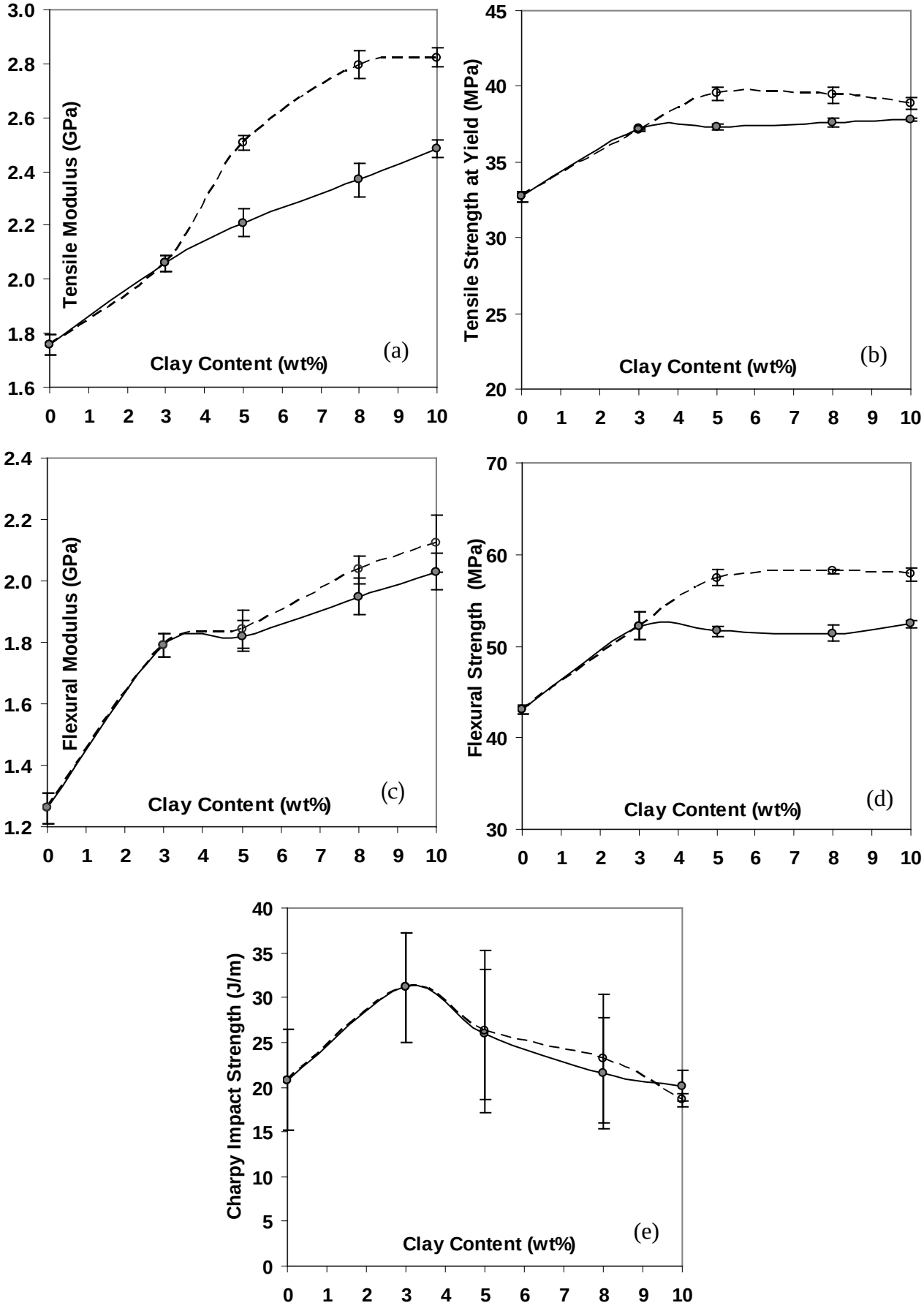
Tensile Modulus (GPa)
Clay Content (wt%)
(a)
Tensile Strength at Yield (MPa)
Clay Content (wt%)
(b)
Flexural Modulus (GPa)
Clay Content (wt%)
(c)
Flexural Strength (MPa)
Clay Content (wt%)
(d)
Charpy Impact Strength (J/m)
Clay Content (wt%)
(e)

Fig.7

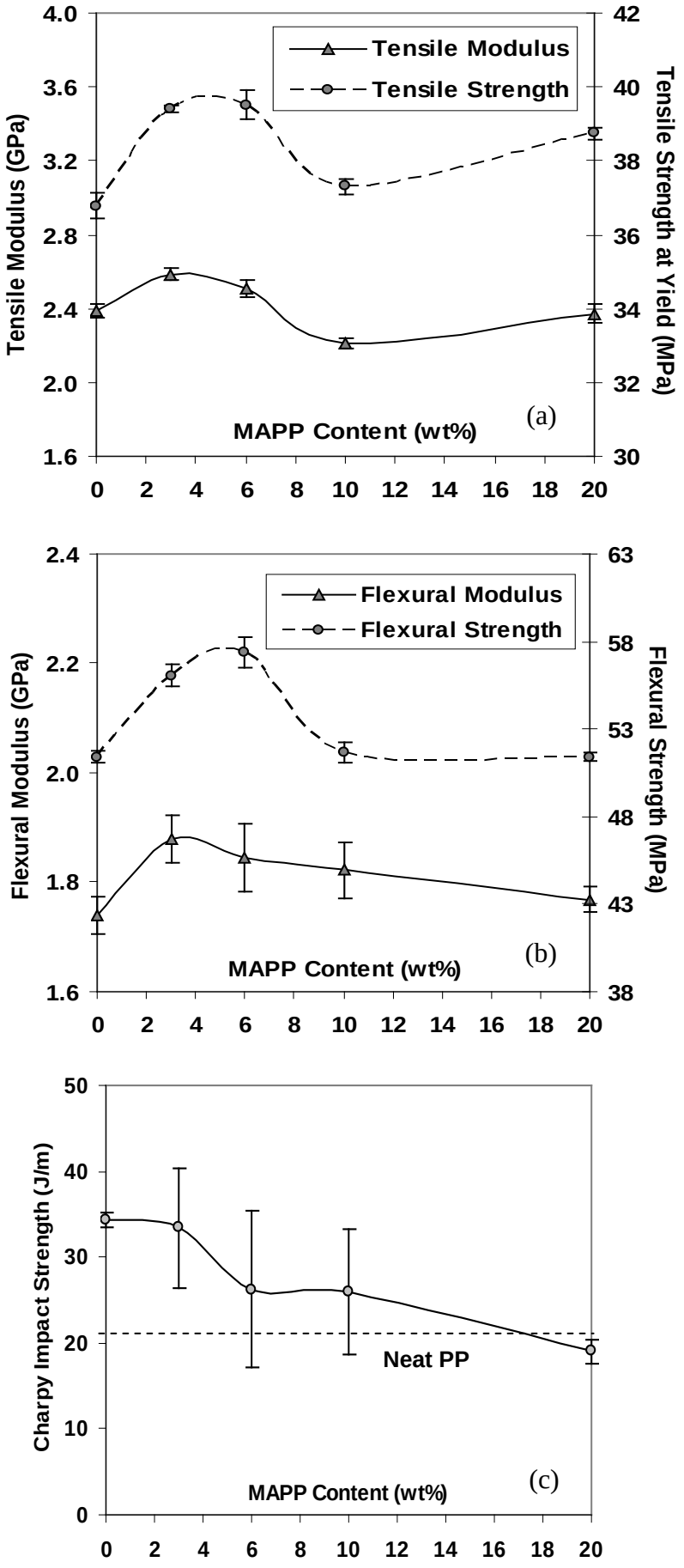
Tensile Modulus
Tensile Strength
Tensile Modulus (GPa)
Tensile Strength at Yield (MPa)
MAPP Content (wt%)
(a)
Flexural Modulus
Flexural Strength
Flexural Modulus (GPa)
Flexural Strength (MPa)
MAPP Content (wt%)
(b)
Charpy Impact Strength (J/m)
Neat PP
MAPP Content (wt%)
(c)

Fig.8

Table 1 Material formulations of PP/clay nanocomposites

Formulation type	Sample name	Composition (wt%)		
		Clay	MAPP	PP
I	Opt1	3	6	91
	Opt2	5	10	85
	Opt3	8	16	76
	Opt4	10	20	70
II	PPNC3 (Opt1)	3	6	91
	PPNC5	5	6	89
	PPNC8	8	6	86
	PPNC10	10	6	84
III	MAPP0	5	0	95
	MAPP3	5	3	92
	MAPP6 (PPNC5)	5	6	89
	MAPP10 (Opt2)	5	10	85
	MAPP20	5	20	75

Table 2 XRD features of DK4 organoclay and corresponding PP/clay nanocomposites

Material type	2θ (1st peak)	d_{001} (nm) (1st peak)	2θ (2nd peak)	d_{002} (nm) (2nd peak)	2θ (3rd peak)	d_{003} (nm) (3rd peak)
DK4 organoclay	2.48°	3.56	4.88°	1.81	7.36°	1.20
Opt1	2.37°	3.73	4.64°	1.90	7.04°	1.25
Opt2	2.39°	3.70	4.69°	1.88	7.06°	1.25
Opt3	2.40°	3.68	4.78°	1.85	7.18°	1.23
Opt4	2.44°	3.62	4.78°	1.85	7.26°	1.22
PPNC3	2.37°	3.73	4.64°	1.90	7.04°	1.25
PPNC5	2.46°	3.58	4.83°	1.83	7.23°	1.22
PPNC8	2.50°	3.53	4.87°	1.81	7.30°	1.21
PPNC10	2.52°	3.50	4.89°	1.81	7.32°	1.21
MAPP0	2.51°	3.52	4.90°	1.80	7.28°	1.21
MAPP3	2.53°	3.49	4.88°	1.81	7.36°	1.20
MAPP6	2.46°	3.58	4.83°	1.83	7.23°	1.22
MAPP10	2.39°	3.70	4.69°	1.88	7.06°	1.25
MAPP20	2.44°	3.62	4.83°	1.83	7.38°	1.20